Biochimica et Biophysica Acta 1827 (2013) 751–760

Contents lists available at SciVerse ScienceDirect

Biochimica et Biophysica Acta

journal homepage: www.elsevier.com/locate/bbabio

Catalytically-relevant electron transfer between two hemes b_L in the hybrid cytochrome bc_1-like complex containing a fusion of *Rhodobacter sphaeroides* and *capsulatus* cytochromes *b*

Monika Czapla, Ewelina Cieluch, Arkadiusz Borek, Marcin Sarewicz, Artur Osyczka *

Department of Molecular Biophysics, Faculty of Biochemistry, Biophysics and Biotechnology, Jagiellonian University, 30-387 Kraków, Poland

ARTICLE INFO

Article history:
Received 18 October 2012
Received in revised form 6 February 2013
Accepted 11 February 2013
Available online 18 February 2013

Keywords:
Cytochrome bc_1
Asymmetric mutagenesis
Fusion hybrid membrane protein
Rhodobacter capsulatus
Rhodobacter sphaeroides
Electron transfer

ABSTRACT

To address mechanistic questions about the functioning of dimeric cytochrome bc_1 new genetic approaches have recently been developed. They were specifically designed to enable construction of asymmetrically-mutated variants suitable for functional studies. One approach exploited a fusion of two cytochromes *b* that replaced the separate subunits in the dimer. The fusion protein, built from two copies of the same cytochrome *b* of purple bacterium *Rhodobacter capsulatus*, served as a template to create a series of asymmetrically-mutated cytochrome bc_1-like complexes (B–B) which, through kinetic studies, disclosed several important principles of dimer engineering. Here, we report on construction of another fusion protein complex that adds a new tool to investigate dimeric function of the enzyme through the asymmetrically mutated forms of the protein. This complex (B_S–B) contains a hybrid protein that combines two different cytochromes *b*: one coming from *R. capsulatus* and the other — from a closely related species, *R. sphaeroides*. With this new fusion we addressed a still controversial issue of electron transfer between the two hemes b_L in the core of dimer. Kinetic data obtained with a series of B_S–B variants provided new evidence confirming the previously reported observations that electron transfer between those two hemes occurs on a millisecond timescale, thus is a catalytically-relevant event. Both types of the fusion complexes (B–B and B_S–B) consistently implicate that the heme-b_L–b_L bridge forms an electronic connection available for inter-monomer electron transfer in cytochrome bc_1.

1. Introduction

Cytochrome bc_1 is an integral component of many biological energy conversion systems. Its role is to oxidize quinol and reduce cytochrome *c* and to couple these reactions with proton translocation across the membrane. This way it contributes to generation of protomotive force used to synthesize ATP. The enzyme is a homodimer in which each monomer consists of three, universally conserved subunits, cytochrome c_1, the FeS subunit and cytochrome *b*. Each monomer embeds two catalytic quinone oxidation/reduction sites located on two opposite sides of the membrane (named the Q_o and Q_i sites) and two chains of cofactors that connect the sites together and also allow them to communicate with quinol pool in the membrane and cytochrome *c* pool outside the membrane (for recent reviews see [1–3]).

The distances between the cofactors in different monomers, as revealed by X-ray crystallography, are large enough to exclude possibility of inter-monomer electron transfer except for one point: a bridge formed by two hemes b_L which in the center of the dimer are at 14 Å edge to edge. This distance appears to be just at the limit of distances between the centers that exchange electrons within micro- to milliseconds, a timescale generally considered to be catalytically-relevant [4].

The revelation about the close distance between two hemes b_L inspired an intense discussion about possible electron transfer between the monomers and its role in a catalytic cycle. An assumption that such electron transfer exists means that the cofactor chains and catalytic sites of two monomers form an H-shaped electron transfer system that all together connects functionally all four catalytic sites of the dimer (see Fig. 5A). Indeed, the possibility of electron transfer between the hemes b_L was so appealing that it became an integral part of several

Abbreviations: FeS subunit, subunit of cytochrome bc_1 containing 2 iron-2 sulfur cluster; *R.*, *Rhodobacter*; EDTA, Ethylenediaminetetraacetic acid; HRP, horseradish peroxidase; B–B complex, cytochrome bc_1-like complex containing fused cytochrome bb in the place of two separate cytochrome *b* subunits in the dimer; B_S complex, cytochrome bc_1 complex containing cytochrome b_S in the place of cytochrome *b*; B_S–B, cytochrome bc_1-like complex containing fused cytochrome b_Sb in the place of two separate cytochrome *b* subunits in the dimer; cytochrome bb, a fusion of two cytochromes *b* of *R. capsulatus*; cytochrome b_S, cytochrome *b* of *R. sphaeroides* expressed in *R. capsulatus* cells; cytochrome b_Sb, a hybrid fusion of cytochrome *b* of *R. sphaeroides* and cytochrome *b* of *R. capsulatus*; B–B strain, MT-RBC1 strain complemented with pMTS1-BBST plasmid used to express the B–B complex; B_S strain, MT-RBC1 strain complemented with pMTS1-BS plasmid used to express the B_S complex; B_S–B strain, MT-RBC1 strain complemented with pMTS1-BSBST plasmid used to express the B_S–B complex

* Corresponding author. Tel.: +48 12 664 6348; fax: +48 12 664 69 02.
E-mail address: artur.osyczka@uj.edu.pl (A. Osyczka).

0005-2728
http://dx.doi.org/10.1016/j.bbabio.2013.02.007

models of the operation of cytochrome bc_1 (see examples in refs [5–7]) and also was considered as providing potential means to diminish levels of unpaired electrons, thus lower risks of superoxide generation by cytochrome bc_1 [6,8,9].

The kinetic evidence that the electron transfer between the hemes b_L takes place on a catalytically-relevant timescale came recently from the studies that used bacterial genetic systems to create asymmetrically-mutated variants suitable for functional studies. One approach was based on a fusion protein that replaced two cytochromes *b* in the dimer [10]. The fusion, built from two copies of the same cytochrome *b* of purple bacterium *Rhodobacter capsulatus*, was used to create a series of asymmetrically-mutated cytochrome bc_1-like complexes (B–B). To examine the path that exclusively relies on the heme b_L–b_L electron transfer, a cross-mutated variant of B–B was used in which the complementary segments of the dimer were cross-inactivated leaving the inter-monomer path as the only way connecting the catalytic sites (see scheme shown in Fig. 5B). Flash-induced electron transfer measurements performed with this mutant revealed that electron transfer between the two hemes b_L takes place on a millisecond timescale [10]. In addition, the functional connection between the catalytic Q_o and Q_i sites in this mutant was confirmed by analysis of its enzymatic activity both in the membranes and in the isolated form [11]. Another genetic approach exploited a two plasmid system with two different tags to generate and analyze the heterodimeric cross-inactivated forms of cytochrome bc_1 of *R. capsulatus* [12]. This study provided independent experimental indications for the existence of the heme b_L–b_L electron transfer.

The two approaches just described, together with a two-plasmid system developed for *Paraccocus denitrificans* [13], are so far the only known systems that allow studying the operation of the dimeric cytochrome bc_1 through asymmetric mutagenesis. In all cases the expression of heterodimers relies on two copies of the same gene that serve as a template for mutagenesis. From the technical point of view this makes those systems challenging in that it requires a special experimental care to guard against genetic recombination to maintain the desired constructs at genetic level (see [14] for discussion on this issue). Here, we present a new system that overcomes this difficulty. The system follows our original strategy of replacing two separate cytochrome *b* subunits in the dimer with a fusion protein, however now instead of fusing two identical cytochromes *b* of *R. capsulatus* we created a hybrid protein combining two different cytochromes *b*: one coming from *R. capsulatus* and the other — from closely related *R. sphaeroides*. With this new fusion we provide further kinetic evidence for the existence of heme b_L–b_L electron transfer on a catalytically-relevant timescale.

2. Materials and methods

2.1. Bacterial strains, growth conditions and plasmids

E. coli (HB101 and DH5α) were grown in liquid or solid Luria–Bertrani (LB) medium supplemented with appropriate antibiotics (ampicillin or kanamycin), at 37 °C. *R. capsulatus* cells were cultivated on liquid or solid mineral-peptone-yeast extract (MPYE) medium supplemented with kanamycin when needed. They were grown at 30 °C in the dark under semiaerobic conditions or in light under anaerobic conditions. Photosynthetic growth abilities were tested on MPYE plates using anaerobic jars (GasPakTM Anaerobe Container System, BD). MT-RBC1, a strain in which the chromosomal copy of *pet*ABC operon has been deleted, was used as a host for expression of cytochrome bc_1 and its derivatives from expression vectors introduced into MT-RBC1 via triparental crosses [15].

The plasmids pPET1-BL [14], pUC-BLST [14], and pBC9 [16] were used as templates for genetic manipulations. The plasmid pMTS1 [15] (carries a *pet*ABC operon coding for three subunits of *R. capsulatus* cytochrome bc_1) and its mutagenized derivatives were used as expression vectors.

2.2. Construction of expression plasmids

The plasmid pMTS1-BS used for expression of B_S complex (cytochrome bc_1 containing *R. capsulatus* FeS and cytochrome c_1 subunits and *R. sphaeroides* cytochrome *b*) was constructed from two plasmids: pPET1-BL and pBC9. The steps of pMTS1-BS construction are described in details in Supplementary data Fig. S1.

The plasmid pMTS1-BSBST used for expression of B_S–B complex (cytochrome bc_1-like complex in which two separate cytochrome *b* subunits in dimer are replaced with a hybrid cytochrome b_Sb built of *R. sphaeroides* and *R. capsulatus* cytochromes *b* fused together) and its mutagenized derivatives containing various combinations of point mutations of cytochrome *b*: G158W, H198N and H212N, were constructed according to description in Supplementary data Fig. S2.

2.3. Isolation of membranes and proteins, electrophoresis and Western blot

The chromatophore membranes were prepared from semiaerobically grown cultures of *R. capsulatus* as described in [17]. Membranes solubilization with n-dodecyl-β-D-maltoside (DDM) and protein purifications were performed as described in [14]. The B_S complex was purified using DEAE-Biogel column (BioRad), while the B_S–B complexes were purified using Strep-tag affinity chromatography (IBA Biotagnology). Sodium dodecyl sulfate polyacrylamide gel electrophoresis (SDS-PAGE) was performed as described in [18]. The Western blot against Strep-tag was performed according to the protocol supplied by IBA with HRP-streptactin.

2.4. Optical and electron paramagnetic resonance spectroscopy and flash-induced electron transfer measurements

Optical spectra for *b*- and *c*-type cytochromes were recorded at room temperature using Shimadzu UV-2450 spectrophotometer. The difference spectra were obtained with samples that were first oxidized by an addition of potassium ferricyanide and then reduced by using either sodium ascorbate or a minimal amount of solid sodium dithionite. Continuous wave electron paramagnetic resonance (EPR) spectra of 2Fe-2S cluster in chromatophores were measured according to the protocol described in [19]. Flash-induced electron transfer of B_S and B_S–B complexes were performed as described in [20]. For the measurements, chromatophore membranes were suspended in 50 mM MOPS buffer pH 7, containing 100 mM KCl, 1 mM EDTA, 3.5 μM valinomycin, and appropriate redox mediators (7 μM 2,3,5,6-tetramethyl-1,4-phenylenediamine, 1 μM phenazine methosulfate, 1 μM phenazine ethosulfate, 5.5 μM 1,2-naphthoquinone, 5.5 μM 2-hydroxy-1,4-naphthoquinone). The samples were poised at an ambient potential of 100 mV. Transient cytochrome *c* and *b* reduction kinetics were followed at 550–540 nm and 560–570 nm, respectively. Inhibitors antimycin A and myxothiazol were used at a final concentration of 7 μM.

3. Results

3.1. Cytochrome b of R. sphaeroides can replace native cytochrome b in R. capsulatus cytochrome bc_1

As prerequisite for experiments of fusing two different cytochromes *b* described in the following sections, we have tested the effect of replacing native cytochrome *b* of *R. capsulatus* cytochrome bc_1 with that coming from the closely related strain, *R. sphaeroides*. To this end we constructed an expression vector pMTS1-BS, which in the place of native *R. capsulatus pet*B gene in *pet*ABC operon contained the gene *fbc*B coding for *R. sphaeroides* cytochrome *b* (Fig. 1). The major steps of pMTS1-BS construction are summarized in Supplementary data Fig. S1.

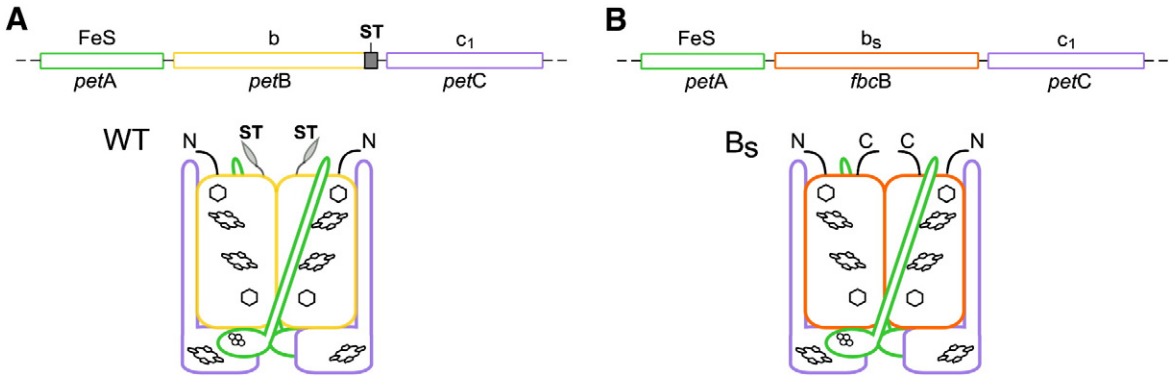

Fig. 1. Schematic representation of operon and subunit composition of native *Rhodobacter capsulatus* cytochrome bc_1 and engineered B_S complex. (A) Native operon *pet*ABC contains three genes coding for three catalytic subunits that assemble as a homodimer: *pet*A for FeS subunit (green), *pet*B for cytochrome *b* subunit (yellow) and *pet*C for cytochrome c_1 (violet). ST — sequence coding for the Strep-tag (gray). (B) In the *pet*ABC operon, *pet*B gene was replaced by *fbc*B gene encoding cytochrome *b* subunit of *R. sphaeroides* bc_1 complex (orange). The expression of this operon resulted in a formation of the dimeric B_S complex in which the cytochrome c_1 and FeS subunits are from *R. capsulatus* while the cytochrome *b* subunit is from *R. sphaeroides* (orange). This cytochrome is named b_S.

We introduced this plasmid to *R. capsulatus* MT-RBC1 strain and found that an appropriately assembled and functional cytochrome bc_1 (named B_S) was expressed in the cells. The absorption redox difference spectra of chromatophore membranes confirmed presence of hemes b and c (peaks at 560 and 550 nm in Fig. 2A, respectively). The isolated from membranes B_S complexes showed similar optical spectra and contained all three catalytic subunits, cytochrome *b*, c_1, and FeS, as seen on SDS-PAGE gels (not shown).

Light-induced electron transfer measurements in chromatophore membranes confirmed that B_S showed typical phases of electron transfer related to the action of the catalytic sites and responded in native-like manner to an addition of specific inhibitors of cytochrome bc_1 (myxothiazol for the Q_o site and antimycin for the Q_i site) (Fig. 2B). From kinetic transients of cytochrome *c* reduction and cytochrome *b* re-oxidation in the absence of inhibitor it is clear that the enzyme is fully operational (both the reduction of cytochrome *c* and the re-oxidation of heme *b* proceed to completion). However the rates of the light-induced reactions were lower, comparing to the respective rates of native cytochrome bc_1, and also the amplitude of heme *b* reduction in the presence of antimycin was smaller (Fig. 2B, B_S vs WT). This indicates that in the presence of this inhibitor the distribution of electrons within the cofactor chains is altered in B_S (see ref. [20]). The reason of these effects is currently unknown but may reflect some structural distortions associated with a necessity to accommodate *R. sphaeroides* cytochrome *b*. For example, the lack of subunit *IV*, which in native cytochrome bc_1 of *R. sphaeroides* naturally interacts with cytochrome *b* subunit [21] but is missing in native cytochrome bc_1 of *R. capsulatus*, and thus is not present in B_S either, may contribute to these effects. (Detailed analysis of B_S is under way and will be a subject of separate studies.) Consistent with the kinetic results, the strain expressing B_S showed Ps + phenotype indicating that this enzyme is functional in vivo.

Based on these results we concluded that cytochrome *b* of *R. sphaeroides* is capable of replacing native cytochrome *b* in *R. capsulatus* cytochrome bc_1, and the engineered B_S retains functional and structural properties of cytochrome bc_1.

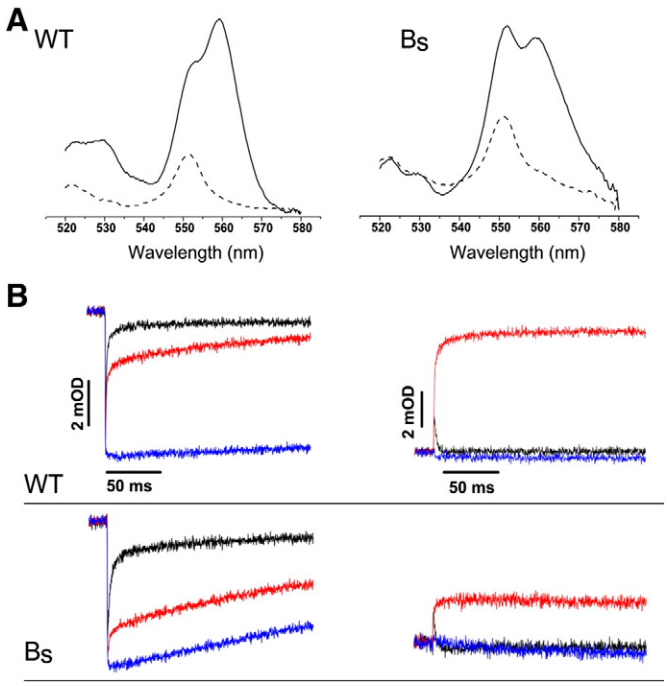

Fig. 2. Spectroscopic and kinetic properties of B_S complex. (A) Reduced *minus* oxidized optical difference spectra of b- and c-type hemes in chromatophore membranes isolated from wild-type (WT) and the B_S strain (B_S). Dithionite *minus* ferricyanide spectra — solid lines, ascorbate *minus* ferricyanide spectra — dashed lines. (B) Light-induced cytochrome *c* oxidation and re-reduction (left panel) and cytochrome *b* reduction and re-oxidation (right panel) of WT and B_S complexes recorded at 550–540 nm and 560–570 nm, respectively, at pH 7 and an ambient potential of 100 mV. Color code: no inhibitor, black; antimycin, red; and myxothiazol, blue. The vertical and horizontal scales of the lower panel are as those of the upper panel shown in the figure.

3.2. Hybrid cytochrome $b_S b$ obtained by fusion of cytochromes b from *R. sphaeroides* and *R. capsulatus* assembles with other core subunits to form B_S–B complex

The fusion of cytochromes *b* from *R. capsulatus* and *R. sphaeroides* was achieved adopting similar strategy that was previously used to fuse two cytochromes *b* of *R. capsulatus* [10]. At genetic level, this strategy requires modification of the expression vector so that the operon coding for cytochrome bc_1 contains cytochrome *b* gene (*pet*B) extended in frame with an additional copy of cytochrome *b* gene. While in our previous work, the two halves of the fusion gene were alike, each containing a sequence of the same *pet*B gene originated from *R. capsulatus* [10], in this work we constructed a fusion gene assembled from two different genes: *fbc*B and *pet*B (Fig. 3). The first half of the fusion gene contained the sequence of *fbc*B from *R. sphaeroides* while the second half contained the sequence of *pet*B from *R. capsulatus* with the sequence encoding Strep-tag at its 3′ end (this fusion gene was named *fbc*B/*pet*B). The other two genes of the operon *pet*ABC, encoding the FeS subunit and cytochrome c_1, were left unchanged. All three genes were expressed using a vector

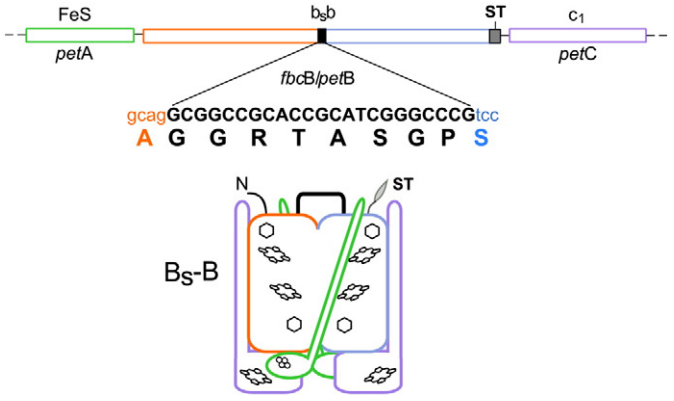

Fig. 3. Operon organization and subunit composition of the fusion hybrid B_S–B complex. In the *pet*ABC operon, the *pet*B gene was replaced by a hybrid fusion gene *fbcB*/*petB* composed of *fbc*B of *R. sphaeroides* and *pet*B of *R. capsulatus* (orange and blue). The remaining genes in the operon are: *pet*A coding for the FeS subunit (green), and *pet*C coding for cytochrome c_1 (violet). The expression of this operon resulted in a formation of the B_S–B complex in which the two cytochrome *b* subunits in the dimer are replaced with hybrid cytochrome b_Sb (a fusion of cytochromes *b* of *R. sphaeroides* and *R. capsulatus*). DNA sequence and amino acid composition of the linker is shown in black. Orange and blue letters indicate the last and the first codons/amino acid residues that were left unchanged in *R. sphaeroides* and *R.capsulatus* gene/protein, respectively. ST — sequence coding for the Strep-tag (gray).

pMTS1-BSBST, which was a derivative of pMTS1 containing *fbc*B/*pet*B in the place of *pet*B gene. The major steps of construction of pMTS1-BSBST are described in Supplementary data Fig. S2.

Fig. 4 summarizes the results of expression of pMTS1-BSBST in MT-RBC1 cells. First, spectroscopic measurements of membranous fractions revealed the presence of redox cofactors characteristic for cytochrome bc_1-type complexes: absorption redox difference spectra showed presence of hemes b and c (peaks at 560 and 550 nm in Fig. 4A, respectively) while EPR showed presence of Rieske protein appropriately interacting with occupants of the Q_o site [22] (characteristic g_x value of the spectrum of Fig. 4B). Second, Western blots revealed the presence of the fusion protein of correct size (two times larger than cytochrome *b*) in the membranes (Fig. 4C). The fusion protein was also clearly visible on SDS-PAGE of complexes isolated from the membranes using affinity chromatography (Fig. 4D). The electrophoretic profile of isolated complexes showed that the fusion protein was accompanied by the two remaining subunits of cytochrome bc_1: cytochrome c_1 and the FeS subunit, consistent with spectroscopic features just described. These results provided first indication that the membranes contained a cytochrome bc_1-like complex built of the hybrid fusion protein (named cytochrome b_Sb) assembled together with cytochrome c_1 and the FeS subunit (the entire complex was named B_S–B). Further kinetic experiments confirmed that B_S–B did assemble in the membranes (see below). In the remaining text the system of expression of B_S–B in *R. capsulatus* cells will be referred as the *sphaer–caps* system. For consistency, the system of expression of B–B described earlier in [10,14] will be named as the *caps–caps* system.

We note that Western blot and Coomassie blue-stained gels revealed also traces of a protein in size corresponding to native cytochrome *b* (Fig. 4C, D). The amount of this cytochrome *b* in relation to the fusion protein was always significantly smaller, as exemplified on gel in Fig. 4D. These results indicate that in addition to the dominant fraction of B_S–B, the membranes contain a small fraction of cytochrome *b* either alone or assembled with cytochrome c_1 and FeS subunits. At present, the origin of this phenomenon is not clear. Given that the fusion constructs are commonly reported to encounter problems with proteolysis upon expression and/or isolation of proteins [23–27], we favor an explanation that in our case it is also a result of partial degradation of protein, especially of a foreign *R. sphaeroides* portion of the fusion protein with retention of the *R. capsulatus* part (this part contains Strep-tag used for Western blot

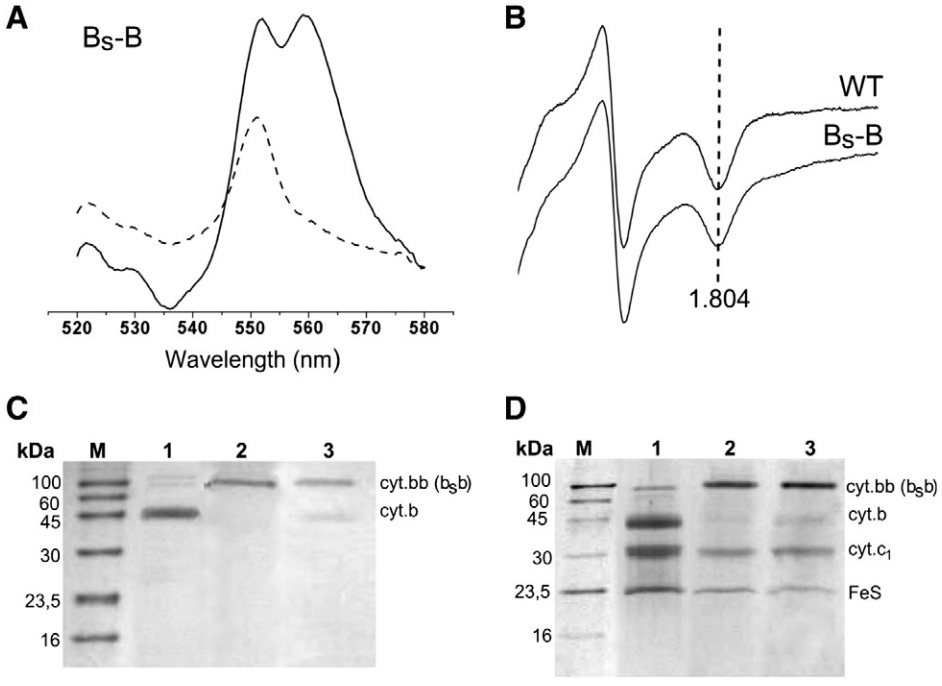

Fig. 4. Spectroscopic properties and Western blot/SDS-PAGE analyses of B_S–B. (A) Optical redox difference spectra of b- and c-type hemes in chromatophore membranes isolated from the B_S–B strain. Dithionite *minus* ferricyanide spectra — solid lines, ascorbate *minus* ferricyanide spectra — dashed lines. (B) X-band continuous wave EPR spectra of the 2Fe-2S cluster of WT and B_S–B complexes in chromatophore membranes. Dotted line shows the position of g_x transition. (C) Western blot against Strep-tag II (IBA Biotagnology) of chromatophore membranes isolated from wild type (lane 1), the B–B strain (lane 2) and the B_S–B strain (lane 3). M, Molecular weight marker. Names cyt. bb and cyt. b_Sb depict the protein shown in line 2 and 3, respectively. (D) Coomassie blue stained SDS-PAGE analysis of complexes isolated using affinity chromatography (Strep-tag) from wild-type (lane 1), the B–B strain (lane 2) and the B_S–B strain (lane 3). M, Molecular weight marker. Names cyt. bb and cyt. b_Sb are the same as in C.

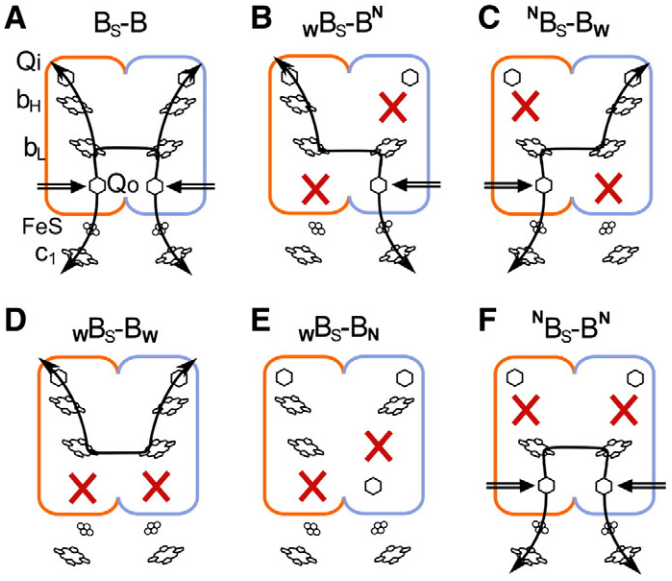

Fig. 5. Symmetric and asymmetric knockout patterns in the fusion hybrid B_S–B complex. (A) B_S–B complex without mutation — four branches for electron transfer are open forming an H-shaped electron transfer system characteristic for the intact wild-type cytochrome bc_1; (B) $_WB_S$–B^N and (C) ^NB_S–B_W — two branches across removed (cross-inactivation) and heme b_L–b_L connection maintained; (D) $_WB_S$–B_W — both lower branches removed; (E) $_WB_S$–B_N — two branches across removed and heme b_L–b_L connection disrupted; (F) ^NB_S–B^N — both upper branches removed (note that this form is drawn schematically but was not obtained as a fusion protein complex). W, N (subscript), and N (superscript) refer to G158W, H198N, and H212N point mutations in cytochrome *b*, respectively. Black arrows indicate functional branches. Black double arrows indicate electron entry point at the Q_o site. Red crosses display distribution of G158W, H198N, and H212N point mutations in B_S–B complexes.

detection and affinity chromatography). At the same time we are certain that this cannot be due to genetic recombination leading to shortening of the fused gene. The results shown in the next paragraphs have demonstrated that the *sphaer–caps* system exhibits high genetic stability.

Our initial attempts to eliminate completely this background of cytochrome *b* have proven that this was not a straightforward task. We did not investigate this issue any further as for the main purpose of this work it was not necessary. We reasoned that as long as B_S–B complex was assembled in the membranes and there was a possibility to perform all appropriate control experiments, the background of cytochrome *b* would not compromise the kinetic experiments that were a subject of present studies.

3.3. B_S–B protein accommodates several point mutations introduced in symmetric and asymmetric patterns

In the next series of experiments, we introduced point mutations to pMTS1–BSBST template repeating the strategy used earlier to create symmetrically and asymmetrically mutated B–B complexes [10] (Fig. 5). The point mutations included G158W to inactivate the Q_o site and the lower branch of the H-shaped electron transfer system [22] and H212N to inactivate the Q_i site and the upper branch of this system [8] (numbering corresponds to the sequence of *R. capsulatus* cytochrome *b*). The asymmetric combinations contained an equivalent of G158W in one half of the hybrid gene and an equivalent of H212N in the other half (to obtain $_WB_S$–B^N or ^NB_S–B_W, Fig. 5B, C). The symmetric combinations contained equivalents of G158W or H212N in both halves of the gene (to obtain $_WB_S$–B_W or ^NB_S–B^N, Fig. 5D, F). Table 1 and Fig. 6 summarize the results of expression of pMTS1–BSBST derivatives containing appropriate mutations in MT-RBC1 strain. Table 1 also compares these results with those obtained previously when the same combinations of mutations were tested with the *caps–caps* system [10,14].

From Table 1 and Fig. 6, it is clear that B_S–B complex containing the fusion protein is assembled in all cases, except for ^NB_S–B^N. Most importantly, both asymmetric combinations $_WB_S$–B^N and ^NB_S–B_W resulted in an assembly of the fusion protein. The *sphaer–caps* system allowed also for an assembly of the complex containing one of the symmetric mutation patterns (i.e. $_WB_S$–B_W). The latter pattern was previously unavailable with the *caps–caps* system, which in general did not tolerate the presence of the same mutation in both halves of the fusion protein [14].

In this work we also tested a new asymmetric pattern $_WB_S$–B_N or $_WB$–B_N (for *sphaer–caps* or *caps–caps* system, respectively) (Fig. 5E). This combination contained G158W in the first half of the fusion protein and an equivalent of H198N introduced in the second half and was specifically designed to perform a series of genetic and kinetic control experiments described in next paragraphs. In cytochrome *b*, mutation H198N replaces one of the histidine ligand to iron of heme b_L with non-competent asparagine and, as previous studies with *R. sphaeroides* have indicated, results in an assembly of the cytochrome bc_1 complex with an impaired Q_o site [28]. This mutation has not been described earlier for *R. capsulatus*, but our initial experiments confirmed that also in this species H198N mutant assembles as cytochrome bc_1 with impaired Q_o site (manuscript in preparation). We thus used H198N and G158W to create a form intended to disable both the Q_o sites, each by a different point mutation. Those two point mutations were separated from each other in DNA sequence of *pet*B, which was important from a genetic point of view for the planned experiments (this separation was one of the reasons for selection of H198N over other mutations in cytochrome *b* that are also known to inactivate the Q_o site but are closer to G158W in sequence).

As Table 1 indicates, the form containing equivalents of H198N and G158W assembled as fusion protein only as $_WB_S$–B_N in the *sphaer–caps* system. For the *caps–caps* system, the results were similar to those previously described for all symmetrically mutated forms (^NB–B^N, $_WB$–B_W) [14].

In general, from the comparison shown in Table 1 it appears that B_S–B have more structural flexibility to accommodate larger number of mutational patterns than B–B. Possibility to analyze those combinations of B_S–B that were previously unavailable with B–B (i.e. $_WB_S$–B_W, $_WB_S$–B_N)

Table 1
Assembly of B–B and B_S–B complexes in *R. capsulatus* cells.

Name of fusion protein (*caps–caps* system)	Assembly of B–B	Name of fusion protein (*sphaer–caps* system)	Assembly of B_S–B
B–B	+	B_S–B	+
$_WB$–B_W	−	$_WB_S$–B_W	+
^NB–B^N	−	^NB_S–B^N	−
$_WB$–B_N	−	$_WB_S$–B_N	+
^NB–B_W	−	^NB_S–B_W	+
$_WB$–B^N	+	$_WB_S$–B^N	+

W, N (subscript), and N (superscript) indicate position of mutation corresponding to G158W, H198N and H212N in cytochrome *b* subunit, respectively. "+" indicates assembly of the complex containing the fusion protein. "−" indicates lack of the fusion protein (for ^NB_S–B^N, $_WB$–B_W, ^NB–B^N, $_WB$–B_N) or the presence of dominant fraction of the complex with unfused protein (for ^NB–B_W) see ref. [14].

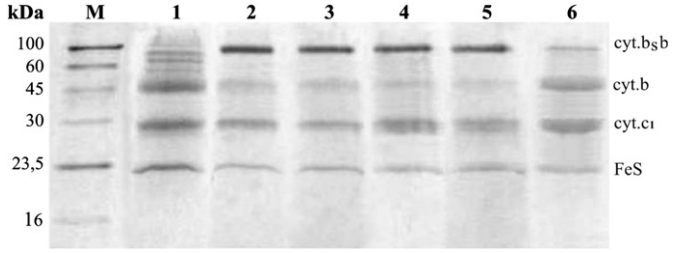

Fig. 6. SDS-PAGE analysis of various B_S–B complexes with knockout mutations isolated using affinity chromatography (Strep-tag). Lanes: M, Molecular weight marker (IBA); 1, wild-type cytochrome bc_1; 2, $_WB_S$–B^N; 3, ^NB_S–B_W; 4, $_WB_S$–B_W; 5, $_WB_S$–B_N; 6, ^NB_S–B^N.

is highly valuable as it offers additional level of control and means to verify conclusions drawn earlier with B–B.

3.4. The sphaer–caps system exhibits high genetic stability

We have previously observed that in the *caps–caps* system, the cells carrying genes coding for B–B did not grow photosynthetically (exhibited Ps− phenotype). However, the photosynthetic growth conditions allowed for selection of revertants. The cells that regained Ps+ phenotype carried plasmids containing only a short version of the gene (corresponding in size to a single copy of *pet*B) (Fig. 7B). The reversions to Ps+ occurred with a frequency of 10^{-3}–10^{-4}, which was estimated from the number of cells that were able to grow photosynthetically at given concentration of cells. The tests involved serial dilutions experiments where the number of colonies that can grow under photosynthetic conditions was compared to the total number of cells equal to the number of cells growing under aerobic conditions (an example of the result for a given concentration of cells is shown in Fig. 7A, top).

Similar tests were now performed for the cells carrying pMTS1–BSBST (used for expression of B_S–B) in the *sphaer–caps* system. First, we checked the cells expressing B_S–B without additional mutations and observed that the number of colonies that grow under photosynthetic and aerobic conditions for given concentrations of the cells was always similar (Fig. 7A, middle). We also found that the cells grown under photosynthetic conditions retained the original plasmid pMTS1–BSBST with intact fused gene *fbc*B/*pet*B and showed no signs of a short copy of the gene (Fig. 7B). Furthermore, the SDS profile of complexes isolated from the membranes of these cells (Fig. 7C, lane 2) indicated that they contained B_S–B complex with fusion protein (the SDS profile of the complexes obtained from the photosynthetic cultures was very similar to that obtained from the semiaerobic cultures, see, lane 3 of Fig. 4D). This all was a first indication that the frequency of genetic recombination in the *sphaer–caps* system is low and that this system is genetically more stable than the *caps–caps* system.

We note that because the cells expressing B_S–B show some background of unfused cytochrome *b* subunit (Fig. 4C, D), the Ps+ phenotype in itself cannot be used as an argument in discussions about possible functionality of B_S–B in vivo. Clearly, other experiments are needed to asses it (such experiments are currently under way).

To further asses genetic stability of the *sphaer–caps* system we analyzed the non-functional $_WB_S$–B_N variant which had two of its Q_o sites disabled by two different mutations positioned in protein sequence 40 amino acids apart (G158W in one half and an equivalent of H198N in the other). In this case, although the mutant cells expressing $_WB_S$–B_N complex were Ps−, as expected, there was a theoretical possibility of homologous recombination between parts of the fusion gene resulting in a sequence that would remove deleterious mutation and restore the functional Q_o site. Those types of recombinant cells

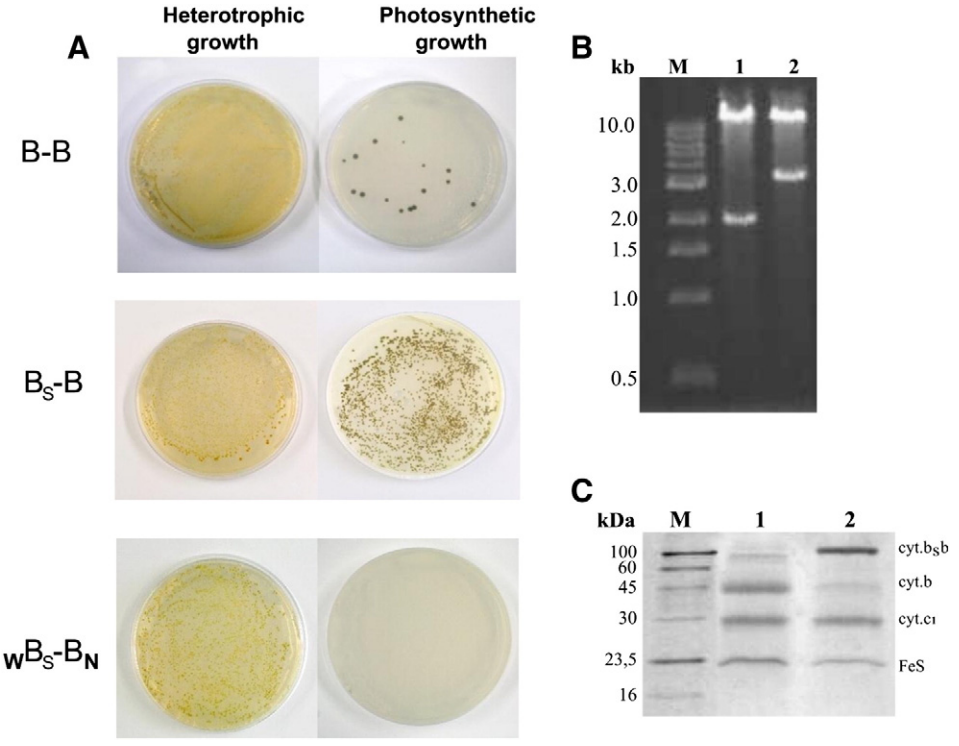

Fig. 7. Effect of photosynthetic selection on strains expressing various fusion proteins. (A) Comparison of heterotrophic and photosynthetic growth of *R. capsulatus* strains expressing B–B (top), B_S–B (middle), $_WB_S$–B_N (bottom). For each strain the same amount of cells was plated for heterotrophic and photosynthetic growth. (B) Restriction analysis of expression plasmids isolated from the B–B and B_S–B strains grown under photosynthetic anaerobic condition (lanes 1 and 2, respectively). The presence of ~3.3 kb DNA fragment indicates that the plasmid bears fusion gene *fbc*B/*pet*B, while ~2 kb DNA fragment corresponds to the native form of gene *pet*B. M, Molecular weight marker. (C) Coomassie blue stained SDS-PAGE analysis of complexes isolated from the B_S–B strain grown under photosynthetic conditions (lane 2) in comparison with wild-type cytochrome bc_1 (lane 1). M, Molecular weight marker.

can be selected by growing the cells under photosynthetic conditions. Remarkably, however, we could not obtain recombinant cells for this mutant even when very high concentrations of cells were tested. As exemplified in Fig. 7A, bottom, all the cells exhibited Ps − phenotype. Based on the serial dilution tests [14] it was estimated that the frequency of recombination is below 10^{-6}. These results provide evidence that the *sphaer–caps* system exhibits high genetic stability. The frequency of reversion in this system is clearly orders of magnitude lower from that estimated for the *caps–caps* system [14]. We note that it also appears to be lower from the frequency of reversions estimated for the alternative two-plasmid system [12].

3.5. Light-induced electron transfer in B_S–B derivatives confirm occurrence of fast electron transfer between two hemes b_L

Fig. 8 compares kinetic traces of light-induced electron transfer in chromatophore membranes containing various forms of B_S–B. In the chromatophores containing B_S–B complex without any additional mutations in the absence of any inhibitors, hemes *c* (c_1 and c_2) of cytochromes *c* were rapidly photo-oxidized then reduced, while heme b_H of cytochrome *b* was rapidly reduced and re-oxidized (Fig. 8A). Antimycin, inhibitor of the Q_i site, greatly diminished heme *c* reduction phase and fully abolished heme *b* re-oxidation phase leaving only its reduction phase. Myxothiazol, inhibitor of the Q_o site, abolished heme *c* reduction phase and also fully abolished heme *b* reduction and re-oxidation phases. From this data it is clear that B_S–B exhibits all phases of electron transfer reminiscent of the functional catalytic Q_o and Q_i sites connected together, as known for the wild-type enzyme and described earlier for B–B [10].

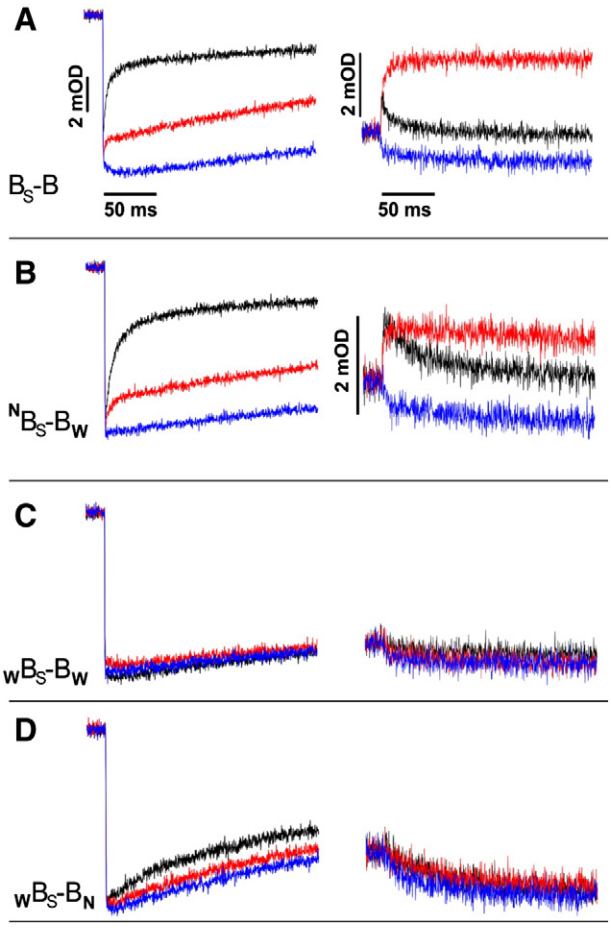

Fig. 8. Light-induced cytochrome *c* oxidation and re-reduction (left panel) and cytochrome *b* reduction and re-oxidation (right panel) in chromatophore membranes containing B_S–B (A), cross-inactivated $^{N}B_S$–B_W (B) and two controls: $_{W}B_S$–B_W and $_{W}B_S$–B_N (C and D, respectively). The traces were recorded at 550–540 nm and 560–570 nm for cytochrome *c* and *b*, respectively, at pH 7 and an ambient potential of 100 mV. Color code: no inhibitor, black; antimycin, red; and myxothiazol, blue. In each panel, the vertical and horizontal scales for cytochrome *c* are as shown in A. The horizontal scales for all cytochrome *b* are as shown in A. The vertical scale for cytochrome *b* in C and D is as in B.

Most significantly, asymmetric $^{N}B_S$–B_W exhibited kinetic behavior consistent with the same mode of operation (Fig. 8B). Again, there was a clear and large phase of antimycin-sensitive reduction of hemes *c*. Heme *b* reduction and re-oxidation phases were antimycin-sensitive: in the absence of any inhibitors heme b_H was rapidly reduced and re-oxidized, while in the presence of antimycin re-oxidation phase was eliminated and only reduction phase was observed. Similar kinetic results were obtained for the mirror asymmetric form $_{W}B_S$–B^{N} (not shown).

In the asymmetric form $^{N}B_S$–B_W the functional connection between the Q_o and Q_i sites can only be accomplished if electrons are transferred between the hemes b_L. This is because in this mutant electrons enter the b chain (reflected as flash-induced reduction of heme b_H) only through one active Q_o site and leave this chain (reflected as flash-induced oxidation of heme b_H) only through one active Q_i site, but each of these two sites is located on a separate half of the fusion protein (Fig. 5C). Thus, to reach the active Q_i site, electrons that entered the enzyme through the active Q_o site must use the path: heme b_L–heme b_L–heme b_H. This also means that when the Q_i site is inactive (in the presence of antimycin), heme b_H cannot be reduced in flash experiments unless the quinol-derived electron is transferred from one heme b_L (that associated with active Q_o site) to another heme b_L (that associated with inactive Q_o site).

A profound antimycin-sensitive phase of cytochrome *c* reduction and the Q_i-site-mediated re-oxidation of heme b_H seen in $^{N}B_S$–B_W indicate that the functional connection between the Q_o and Q_i sites is preserved in this mutant. At the same time, the reduction of heme b_H in the presence of antimycin confirms that this heme is reducible by electrons coming from the active Q_o site. We note that consistent with hemes *c* and *b* reduction/oxidation kinetics, $^{N}B_S$–B_W displayed all cytochrome bc_1-related phases of carotenoid band shifts typical for native cytochrome bc_1 confirming full turnover of the cross-inactivated enzyme in the absence of any inhibitors (not shown). Thus, in light of the above considerations, kinetic traces of the asymmetric $^{N}B_S$–B_W clearly indicate that electron transfer between two hemes b_L must take place on catalytically-relevant timescale. This result is fully consistent with our earlier demonstration of existence of heme b_L–b_L electron transfer reported for cross-inactivated $_{W}B$–B^{N} constructed using the *caps–caps* fusion system [10].

We note that re-reduction of cytochromes *c* in the absence of inhibitors reaches similar level in both $^{N}B_S$–B_W and B_S–B, but at the same time the amplitude of heme b_H reduction in $^{N}B_S$–B_W in the presence of antimycin is smaller comparing to the respective amplitude of B_S–B (Fig. 8B and A). This indicates that, in the post-flash redistribution, electrons equilibrate on cofactors chains to the same final levels in $^{N}B_S$–B_W and B_S–B as long as the Q_o and Q_i sites communicate with the quinone and cytochrome *c* pools. On the other hand, when the outflow of electrons through the Q_i site is blocked by antimycin the final distribution of electrons is different and reduction of heme b_H in $^{N}B_S$–B_W is less complete. At this stage deciding what causes this shift in the final equilibrium is difficult, however this result should not be considered unexpected, especially in light of similar changes in electron distribution observed in antimycin-inhibited cytochrome bc_1 when a barrier for a particular electron transfer reaction was specifically modified [20].

Fig. 8C, D show the results of the controls that involved two fusion forms designed to have heme b_L–b_L electron transfer eliminated: $_{W}B_S$–B_W and $_{W}B_S$–B_N (Fig. 5D and E, respectively). These controls deserve particular attention as, for reasons discussed earlier in [14], they were not previously available with the *caps–caps* fusion system.

In $_{W}B_S$–B_W, no kinetic phases of heme *c* reduction or heme *b* reduction and re-oxidations were observed (Fig. 8C). Furthermore, addition of either antimycin or myxhotiazol had no effect on the kinetic traces. These results are similar to the effects of G158W [10,22] and report that both the Q_o sites in $_{W}B_S$–B_W are inactive. $_{W}B_S$–B_W demonstrates that the complex containing the fusion protein can be fully inactivated when the Q_o-site-inactivating mutation is present in both of its halves.

Kinetic traces recorded for the second control, $_{W}B_S$–$B_{N,}$ are shown in Fig. 8D. The heme *c* reduction phase was almost fully suppressed (we note that the residual cytochrome *c* reduction kinetics seen in the absence of any inhibitors must have come from the half of $_{W}B_S$–B_N containing the equivalent of H198N, as we also observed such residual activity in the H198N mutant) and there were no signs of any phases of heme *b* reduction or re-oxidation. Furthermore, the traces recorded for heme b_H were not sensitive to antimycin or myxhotiazol. Clearly, $_{W}B_S$–B_N shows no signs of functional connection between the Q_o and Q_i sites nor electron transfer between two hemes b_L. We emphasize that the kinetic traces of $_{W}B_S$–B_N are clearly different from those of $^{N}B_S$–B_W (Fig. 8D vs B).

The form $_{W}B_S$–B_N, adds to $_{W}B_S$–B_W as another version of control with both of the Q_o sites inactivated (Fig. 5D, E). But in the case of $_{W}B_S$–B_N, unlike in $_{W}B_S$–$B_{W,}$ there exists a possibility of genetic recombination between parts of the fusion gene to obtain pseudo-native form of the enzyme. Occurrence of such reversions at significant level would manifest itself as a background of native-like kinetic traces visible in flash-induced electron transfer measurements. The results obtained with $_{W}B_S$–B_N clearly demonstrate that this is not the case. The lack of any background of native-like kinetics in chromatophores containing $_{W}B_S$–B_N is consistent with the observation that the *sphaer–caps* system exhibits high genetic stability, thus recombinations between parts of the fused gene that would obscure the kinetic results do not occur.

Fig. 5F presents schematically the cofactor pattern in the mutant allowing to test the conditions when the active Q_o site mediates reduction of heme b_L but further electron transfer to heme b_H is prevented. Although such a mutant was not obtained as fusion protein complex (see Fig. 6, lane 6), the characteristic light-induced kinetic transients of the corresponding b_H knockout (cytochrome bc_1 mutant lacking both hemes b_H) [8] are available for comparison with the transients of $^{N}B_S$–B_W. As described previously [10], and also shown in Fig. S3A, the b_H knockout does not exhibit profound antimycin-sensitive phase of cytochrome *c* reduction present in wild-type cytochrome bc_1 (Fig. 2B) and in $^{N}B_S$–B_W (Fig. 8B). The b_H knockout neither shows heme b_H reduction/re-oxidation phases in the absence of inhibitors, nor heme b_H reduction in the presence of antimycin (Fig. S3B), as observed at 560–570 nm in wild-type cytochrome bc_1 (Fig. 2B) and in $^{N}B_S$–B_W (Fig. 8B). The involvement of heme b_L in the b_H knockout can be seen as antimycin-insensitive reduction phase at 566–573 nm (Fig. S3C). The clear differences between the kinetic traces of the b_H knockout with that of $^{N}B_S$–B_W rule out the possibility that the latter ones result from electron transfer reactions involving just heme b_L without participation of heme b_H (and the Q_i site in the absence of inhibitors).

To sum up the results of control experiments, the kinetic traces recorded for two control fusion forms $_{W}B_S$–B_W and $_{W}B_S$–B_N and for the b_H knockout show no signs of functional connection between the catalytic Q_o and Q_i sites, nor the heme b_H reduction/reoxidation reminiscent of heme b_L–b_L electron transfer (Fig. 8C, D). This further substantiates the conclusion that the kinetic traces of the cross-inactivated asymmetric form $^{N}B_S$–B_W (Fig. 8B) do reveal heme b_L–b_L electron transfer and functional connection between the catalytic sites.

4. Discussion

Our earlier work has shown that a genetic approach of fusing two cytochrome *b* subunits in cytochrome bc_1 offers an attractive opportunity to address crucial bioenergetic questions related to the mechanisms of operation of this enzyme. This in particular concerned controversial issues of possible allostery within the dimeric complex and possibility of communication between the monomers. Experimental results addressing these points have demonstrated that monomers operate independently, but at the same time — can exchange electrons using the electron-transfer bridge formed by two hemes b_L in the core of the dimer [10,11,14].

Mechanistic conclusions were drawn from kinetic analysis of the mutants containing a fusion protein (cytochrome bb) assembled with other core subunits to form cytochrome bc_1-like complex named B–B. The point mutations introduced to cytochrome bb enabled inactivation of individual segments of cofactor chains in various symmetric and asymmetric combinations, exposing various electron transfer paths within B–B for kinetic testing. The path that specifically exposed the electron transfer between two hemes b_L was identified in the asymmetric form $_{W}B$–B^N, in which the complementary parts of the fusion protein were cross-inactivated [10].

From the protein engineering point of view this fusion system (referred in this paper as the *caps–caps* system) came as a remarkable example of flexibility within the whole protein expression and assembly system, which clearly was able to adopt itself to accommodate B–B and several of its mutant derivatives. Because, however, the fusion was based on the two copies of the same gene, the risk of genetic recombination (to remove one copy of a gene or exchange complementary fragments of a gene) imposed a necessity of experimental care to implement protocols that ensured that samples used for kinetic analysis were devoid of unwanted background of recombined proteins. This present work provides an attractive alternative template for asymmetric mutagenesis: a cytochrome bc_1-like complex with a new fusion protein expressed from a gene of improved genetic stability. This new system allowed us to obtain a whole family of mutants that included the cross-inactivated variants together with an extended set of control forms to further analyze electronic communication between two hemes b_L.

The system was based on a fusion of two cytochromes *b*, one coming from *R. sphaeroides* and the other from *R. capsulatus* (the *sphaer-caps* system). Because the new fusion comprised two different genes, the *sphaer–caps* system turned out to be genetically more stable than the *caps–caps* system. Indeed, 17.6% of difference between the two genes in the *sphaer–caps* system appeared sufficient to lower the frequency of recombination between the genes [29,30] orders of magnitude in comparison to the *caps–caps* system. At the same time, the structure of those two closely related cytochromes is very similar [31,32] (90.4% of similarity based on primary sequence) and, as we have shown here, not only cytochrome *b* of *R. sphaeroides* can replace native cytochrome *b* in *R. capsulatus* cytochrome bc_1, but also hybrid cytochrome b_Sb (a fusion of *R. sphaeroides* and *R. capsulatus* cytochromes *b*) assembled with other subunits in membranes of *R. capsulatus* cells to form a hybrid cytochrome bc_1-like complex. This latter complex, named B_S–B, corresponds to the previously described B–B [10].

Using B_S–B as a template we prepared the cross-inactivated variants $^{N}B_S$–B_W and $_{W}B_S$–B^N which repeated the asymmetric combination of mutations in $_{W}B$–B^N originally used to test the electron transfer between the two hemes b_L. In addition, we prepared the control forms $_{W}B_S$–B_W and $_{W}B_S$–B_N, which had both of the Q_o sites of the complex inactivated by mutations and thus allowed us to test the conditions when electron transfer between two hemes b_L was not possible within the fusion protein.

The flash-induced experiments performed with $^{N}B_S$–B_W and $_{W}B_S$–B^N showed the presence of kinetic phases reminiscent of the functional connection between the Q_o and Q_i sites. In addition, these experiments revealed reduction of heme b_H in the presence of antimycin. As all these reactions in those mutants can only be accomplished if the heme b_L–b_L electron transfer takes place, it is clear that the kinetic traces proved that these two hemes exchange electrons on a catalytically-relevant

timescale. $^{N}B_S$–B_W and $_{W}B_S$–B^N demonstrated this reaction in the same manner as the previously described $_{W}B$–B^N [10].

On the other hand, the traces of $_{W}B_S$–B_W and $_{W}B_S$–B_N showed neither signs of functional connection between the Q_o and Q_i sites nor signs of reduction of heme b_H in the presence of antimycin, confirming that the heme b_L–b_L electron transfer does not occur in those two mutants. The observation that the kinetic traces of those two controls clearly differ from the traces of cross-inactivated $^{N}B_S$–B_W and $_{W}B_S$–B^N further substantiated the conclusion that the latter ones did reveal heme b_L–b_L electron transfer.

The lack of electron transfer between two hemes b_L in kinetic traces of $_{W}B_S$–B_N deserves particular emphasis, as this is a variant in which the recombination between the parts of fusion gene to restore the functional Q_o site was theoretically possible. Such recombination was described recently by Hong et al. [33] who constructed similar types of mutants $_{N}B$–B^N or ^{N}B–B_N in *R. sphaeroides* cells (in those forms the complex was fully inactivated by mutations H198N and H212N) and observed that they grew photosynthetically. As the photosynthetic growth in those cases must have come from the reverted forms that were effectively selected during photosynthetic cultivation, the authors assumed that similar reversions occurred in the cross-inactivated forms used to test heme b_L–b_L electron transfer. Based on this assumption they raised concern that our kinetic traces of cross-inactivated $_{W}B$–B^N [10] did not reveal heme b_L–b_L electron transfer but rather originated from the pseudo-native contaminants. The results presented here do not support this view. The cells expressing $_{W}B_S$–B_N did not grow photosynthetically and the estimated frequency of reversion was very low. Consistent with this behavior, the kinetic traces of $_{W}B_S$–B_N showed no signs of native-like activity. Yet the kinetic traces of cross-inactivated $^{N}B_S$–B_W matched the traces recorded earlier for the $_{W}B$–B^N. Clearly, the traces of all our cross-inactivated forms revealed electron transfer between the hemes b_L. It follows that our original kinetic experiments with $_{W}B$–B^N that were prepared using the *caps–caps* system [10] were free of any pseudo-native contaminants despite the fact that recombination frequency was larger in this system comparing to the *sphaer–caps* system.

It should be emphasized that the effect of selection of cells that expressed unfused cytochrome *b* in *R. sphaeroides* under photosynthetic conditions described in ref. [33] is consistent with our observations made for the *caps–caps* system [14]. However, we do not share a view that the photosynthetic selection in these cases reflects in vivo enforcement for monomeric electron transfer, as suggested [33]. While various reasons can be envisaged for this selection (see discussion in ref. [14]), it is clear that it took place irrespective of whether the original mutations within the fusion gene enforced the inter-monomer electron transfer within B–B or not.

It should also be emphasized that the reported by Hong et al. difficulties with interpretation of kinetic experiments [33] originate from the fact that they used photosynthetic growth conditions selecting recombined proteins to prepare the samples for kinetic analysis. We, on the other hand, specifically avoided this type of selection in our preparations.

The successful expression of hybrid cytochrome b_Sb and its assembly with other core subunits to form B_S–B adds to B–B as another remarkable example of the overall structural plasticity of cytochrome bc_1 design and a flexibility within the whole protein expression and assembly system (see [34] for discussion of this issue). However, like in the case of B–B and its derivatives, some distortions from the native structure cannot be ruled out. In this context, one may wonder how much these proteins, which all should undoubtedly be treated as model proteins, resemble native cytochrome bc_1. The biochemical, spectroscopic and kinetic properties of these proteins (in particular the occurrence of all of the characteristic kinetic phases of electron transfer) allow us to be confident that the overall mode of operation follows the catalytic cycle of native cytochrome bc_1. The fact that heme b_L–b_L electron transfer was confirmed independently by the asymmetric forms of the cytochrome bc_1-like fusion complexes coming from two different genetic systems (*caps–caps* and *sphaer–caps*) provides strong evidence in support of the notion that the heme–b_L–b_L bridge forms an electronic connection available for inter-monomer electron transfer in cytochrome bc_1.

The experimental evidence for the electron transfer between hemes b_L emerging from our studies and supported by other independent investigations [12] opens doors to discussions about the physiological significance of the intermonomer electron transfer for cytochrome bc_1 operating in living cells. In this respect, one of the crucial aspects that needs detailed investigation concerns the ratio of intra-monomer vs inter-monomer electron transfer [1,9,35]. This ratio is likely to change in response to the changes in redox conditions and/or changes in the membrane potential. In addition, the ratio might be affected by certain mutations that inactivate or impair parts of the protein and are associated with the process of accumulation of mitochondrial mutations occurring in mitochondrially-coded cytochrome *b* subunit. Future studies with asymmetrically mutated forms of cytochrome bc_1 should provide information on those and other related issues to advance our general understanding on the operation of this complex enzyme.

Acknowledgements

This work was supported by The Wellcome Trust International Senior Research Fellowship (095078/Z/10/Z) and Ministry of Science and Higher Education grant (NN301032339) to AO.

Appendix A. Supplementary data

Supplementary data to this article can be found online at http://dx.doi.org/10.1016/j.bbabio.2013.02.007.

References

[1] W.A. Cramer, S.S. Hasan, E. Yamashita, The Q cycle of cytochrome *bc* complexes: a structure perspective, Biochim. Biophys. Acta 1807 (2011) 788–802.
[2] D.M. Kramer, W. Nitschke, J.W. Cooley, The cytochrome bc_1 and related *bc* complexes: the Rieske/cytochrome *b* complex as the functional core of a central electron/proton transfer complex, in: N. Hunter, F. Daldal, M.C. Thurnauer, J.T. Beatty (Eds.), The purple phototrophic bacteria, Springer, The Netherlands, (2009) 451–473.
[3] E.A. Berry, D.-W. Lee, L.-S. Huang, F. Daldal, Structural and mutational studies of the cytochrome bc_1 complex, in: N. Hunter, F. Daldal, M.C. Thurnauer, J.T. Beatty (Eds.), The purple phototrophic bacteria, Springer, The Netherlands, 2009, pp. 425–450.
[4] C.C. Page, C.C. Moser, X. Chen, P.L. Dutton, Natural engineering principles of electron tunneling in biological oxidation–reduction, Nature 402 (1999) 47–52.
[5] J.W. Cooley, D.-W. Lee, F. Daldal, Across membrane communication between the Q_o and Q_i active sites of cytochrome bc_1, Biochemistry 48 (2009) 1888–1899.
[6] R. Covian, B.L. Trumpower, Regulatory interactions in the dimeric cytochrome bc_1 complex: the advantages of being a twin, Biochim. Biophys. Acta 1777 (2008) 1079–1091.
[7] A.Y. Mulkidjanian, Activated Q-cycle as a common mechanism for cytochrome bc_1 and cytochrome b_6f complexes, Biochim. Biophys. Acta 1797 (2010) 1858–1868.
[8] A. Osyczka, C.C. Moser, F. Daldal, P.L. Dutton, Reversible redox energy coupling in electron transfer chains, Nature 427 (2004) 607–612.
[9] W.A. Rutherford, A. Osyczka, F. Rappaport, Back-reactions, short-circuits, leaks and other energy wasteful reactions in biological electron transfer: redox tuning to survive life in O_2, FEBS Lett. 586 (2012) 603–616.
[10] M. Świerczek, E. Cieluch, M. Sarewicz, A. Borek, C.C. Moser, P.L. Dutton, A. Osyczka, An electronic bus bar lies in the core of cytochrome bc_1, Science 329 (2010) 451–454.
[11] M. Czapla, A. Borek, M. Sarewicz, A. Osyczka, Enzymatic activities of isolated cytochrome bc_1-like complexes containing fused cytochrome *b* subunits with asymmetrically inactivated segments of electron transfer chains, Biochemistry 51 (2012) 829–835.
[12] P. Lanciano, D.-W. Lee, H. Yang, E. Darrouzet, F. Daldal, Intermonomer electron transfer between the low-potential hemes of cytochrome bc_1, Biochemistry 50 (2011) 1651–1663.
[13] M. Castellani, R. Covian, T. Kleinschroth, O. Anderka, B. Ludwig, B.L. Trumpower, Direct demonstration of half-of the sites reactivity in the dimeric cytochrome bc_1 complex, J. Biol. Chem. 285 (2010) 502–510.
[14] M. Czapla, A. Borek, M. Sarewicz, A. Osyczka, Fusing two cytochromes *b* of *Rhodobacter capsulatus* cytochrome bc_1 using various linkers defines a set of protein templates for asymmetric mutagenesis, Protein Eng. Des. Sel. 25 (2012) 15–25.

[15] E. Atta-Asafo-Adjei, F. Daldal, Size of the amino acid side chain at position 158 of cytochrome *b* is critical for an active cytochrome bc_1 complex and for photosynthetic growth of *Rhodobacter capsulatus*, Proc. Natl. Acad. Sci. U. S. A. 88 (1991) 492–496.
[16] C.-H. Yun, R. Beci, A.R. Crofts, S. Kaplan, R.B. Gennis, Cloning and DNA sequencing of the *fbc* operon encoding the cytochrome bc_1 complex from *Rhodobacter sphaeroides*. Characterization of *fbc* deletion mutants and complementation by a site-specific mutational variant, Eur. J. Biochem. 194 (1990) 399–411.
[17] M.B. Valkova-Valchanova, A.S. Saribas, B.R. Gibney, P.L. Dutton, F. Daldal, Isolation and characterization of a two-subunit cytochrome b-c_1 subcomplex from *Rhodobacter capsulatus* and reconstitution of its ubihydroquinone oxidation (Q_o) site with purified Fe-S protein subunit, Biochemistry 37 (1998) 16242–16251.
[18] A. Osyczka, P.L. Dutton, C.C. Moser, E. Darrouzet, F. Daldal, Controlling the functionality of cytochrome c_1 redox potentials in the *Rhodobacter capsulatus* cytochrome bc_1 complex through disulfide anchoring of a loop and a β-branched amino acid near the heme-ligating methionine, Biochemistry 40 (2001) 14547–14556.
[19] M. Sarewicz, M. Dutka, W. Froncisz, A. Osyczka, Magnetic interactions sense changes in distance between heme b_L and iron-sulfur cluster in cytochrome bc_1, Biochemistry 48 (2009) 5708–5720.
[20] E. Cieluch, K. Pietryga, M. Sarewicz, A. Osyczka, Visualizing changes in electron distribution in coupled chains of cytochrome bc_1 by modifying barrier for electron transfer between the FeS cluster and heme c_1, Biochim. Biophys. Acta 1797 (2010) 296–303.
[21] S.-C. Tso, S.K. Shenoy, B. Quinn, L. Yu, Subunit IV of cytochrome bc_1 complex from *Rhodobacter sphaeroides*, J. Biol. Chem. 275 (2000) 15287–15294.
[22] H. Ding, C.C. Moser, D.E. Robertson, M.K. Tokito, F. Daldal, P.L. Dutton, Ubiquinone pair in the Q_o site central to the primary energy conversion reactions of cytochrome bc_1 complex, Biochemistry 34 (1995) 15979–15996.
[23] M. Jahic, M. Gustavsson, A.-K. Jansen, M. Mertinelle, S.-O. Enfors, Analysis and control of proteolysis of a fusion protein in *Pichia pastoris* fed-batch processes, J. Biotechnol. 102 (2003) 45–53.
[24] D.-W. Lee, Y. Oztruk, A. Mamedova, A. Osyczka, J.W. Cooley, F. Daldal, A functional hybrid between the cytochrome bc_1 complex and its physiological membrane-anchored electron acceptor cytochrome c_y in *Rhodobacter capsulatus*, Biochim. Biophys. Acta 1757 (2006) 346–352.
[25] D.-W. Lee, Y. Ozturk, A. Osyczka, J.W. Cooley, F. Daldal, Cytochrome bc_1-c_y fusion complexes reveal the distance constraints for functional electron transfer between photosynthetic components, J. Biol. Chem. 283 (2008) 13973–13982.
[26] H. Hellebust, A. Veide, S.-O. Enfors, Proteolytic degradation of fused protein A-β-galactosidase in *Escherichia coli*, J. Biotechnol. 7 (1988) 185–197.
[27] F. Baneyx, G. Georgiou, In vivo degradation of secreted fusion proteins by the *Escherichia coli* outer membrane protease OmpT, J. Bacteriol. 172 (1990) 491–494.
[28] S. Yang, H.-W. Ma, L. Yu, C.A. Yu, On the mechanism of quinol oxidation at the Q_p site in the cytochrome bc_1 complex, J. Biol. Chem. 283 (2008) 28767–28776.
[29] M. Vulic, F. Dionisio, F. Taddei, M. Radman, Molecular keys to speciation: DNA polymorphism and the control of genetic exchange in enterobacteria, Proc. Natl. Acad. Sci. U. S. A. (1997) 9763–9767.
[30] S. Stambuk, M. Radman, Mechanism and control of interspecies recombination in *Escherichia coli*. I. Mismatch repair, methylation, recombination and replication functions, Genetics 150 (1998) 533–542.
[31] E.A. Berry, L.-S. Huang, L.K. Saechao, N.G. Pon, M.B. Valkova-Valchanova, F. Daldal, X-ray structure of *Rhodobacter capsulatus* cytochrome bc_1: comparison with its mitochondrial and chloroplast counterparts, Photosynth. Res. 81 (2004) 251–275.
[32] L. Esser, M. Elberry, F. Zhou, C.A. Yu, D. Xia, Inhibitor-complexed structures of the cytochrome bc_1 from the photosynthetic bacterium *Rhodobacter sphaeroides*, J. Biol. Chem. 283 (2008) 2846–2857.
[33] S. Hong, V. Doreen, A.R. Crofts, Inter-monomer electron transfer is too slow to compete with monomeric turnover in bc_1 complex, Biochim. Biophys. Acta 1817 (2012) 1053–1062.
[34] M. Czapla, M. Sarewicz, A. Osyczka, Fusing proteins as an approach to study bioenergetic enzymes and processes, Biochim. Biophys. Acta 1817 (2012) 1847–1851.
[35] V.P. Shinkarev, C.A. Wraight, Intermonomer electron transfer in the bc_1 complex dimer is controlled by the energized state and by impaired electron transfer between low and high potential hemes, FEBS Lett. 581 (2007) 1535–1541.